Overstrength of Shear Links in Eccentric Braces

G. Della Corte
Department of Stuctural Engineering, University of Naples "Federico II", Naples, Italy

M. D'Aniello & R. Landolfo
Department of Constructions and Mathematical Methods in Architecture, University of Naples "Federico II", Naples, Italy

15 WCEE
LISBOA 2012

SUMMARY:
The paper presents a study on shear link overstrength, which is defined as the ratio between the peak inelastic and the yield strength. Three basic parameters are devised as generally influencing shear overstrength: (i) axial forces acting on the link, (ii) the ratio of link flange over web area and (iii) the ratio between link length and cross section depth. The study presented does not consider the case of axial forces directly applied to the link, but the tensile axial forces developing as a consequence of axial restraints are taken into account. Numerical analysis of finite element (FE) models has been carried out in order to ascertain the combined influence of these factors on the plastic overstrength. A simple analytical model is proposed on the basis of FE model analysis results. The analytical predictions are compared with results of available experimental test results, showing satisfactory agreement.

Keywords: Eccentric bracing; FE model; link; overstrength; shear

1. INTRODUCTION

In steel Eccentric Braced Frames (EBFs) short links are the elements devoted to dissipate the earthquake input energy through shear cyclic plastic deformation. A good estimate of the level of hardening developing prior than buckling or fracture phenomena produce strength degradation is essential at the design stage for a reliable application of capacity design principles. Former tests on shear links were carried out in the 1980s (Roeder and Popov 1978, Hjelmstad and Popov 1983, Popov and Malley 1983, Kasai and Popov 1986, Ricles and Popov 1987, Popov and Engelhardt 1988), showing failure in the form of local shear buckling of panel zones at link ends, ultimately leading to fracture because of excessive local plastic deformation. More recent experimental results (Okazaki and Engelhardt 2007), on modern shear links made of higher strength materials, showed a different type of failure, with web fracture occurring prior than any buckling phenomena taking place. Possible explanations of this new type of behaviour were the different welding processes and stiffener details, as respect to those implemented in the 1980s (Okazaki and Engelhardt 2007). The new type of failure mode exhibited in the tests reported by Okazaki and Engelhardt (2007) was also responsible of reduced deformation capacity of shear links, which did not meet the standard requirement of 0.08 rad as minimum available plastic rotation under conventional cyclic loading history. However, within the research carried out by Richards and Uang (2006), a new testing protocol was purposely developed for shear links, which resulted in a larger number of small-amplitude deformation cycles and a smaller number of large-amplitude deformation cycles. The modern shear links satisfied the 0.08 rad minimum plastic rotation requirement when the new loading protocol was considered, even though failure occurred almost always by web fracture before buckling. Notwithstanding this new type of ultimate failure mode, the peak inelastic strength was measured to be in the range 1.4-1.5 times the yield strength of the link web, thus confirming results from the former tests carried out in the 1980s.
On the contrary, significantly larger values of plastic over-strength have been shown by links tested by McDaniel *et al*. (2003) and Dusicka *et al*. (2010). In particular, McDaniel *et al*. (2003) carried out cyclic tests on two full-scale built-up shear links and found that the over-strength factors were 1.83

and 1.94. Dusicka *et al*. (2010) performed experimental tests on shear links made of both conventional and special high-strength and low-strength steels, concluding that the over-strength factor may range from 1.50 to 4.00, with a value of about 2.2 obtained in the case of ordinary carbon steel.
Full-scale tests of a real two-story reinforced concrete structure equipped with Y-shaped eccentric braces were carried out using both a European wide-flange shape (HE type) and a purposely designed built-up cross-section (D'Aniello 2006, Mazzolani *et al*. 2009). Even if no direct measure was taken of the link shear force vs. rotation relationship, test results and their back analysis clearly indicate that values of shear over-strength appreciably larger than 1.5 were exhibited at link plastic rotations of about 0.08 rad.
This paper presents a theoretical investigation about the plastic shear overstrength of short links made of typical European shapes (HE and IPE). Different end restraint conditions are examined. The theoretical investigation is based on the results of finite element (FE) model simulations, but a simple analytical model is also presented for computing the plastic overstrength in such cases. The FE model has been verified by comparison with some experimental test results from the literature.

2. FINITE ELEMENT MODELS

2.1. Modelling assumptions

Finite element models have been developed using ABAQUS 6.10. The shell element type "S4R" has been used, with four nodes and six degrees of freedom per node. The geometry of each shell model corresponded to the centerline dimensions of a prototype link. Mesh refinement studies were conducted to determine the required level of refinement. Steel yielding has been modelled by means of the von Mises yield criterion. Plastic hardening was represented using a nonlinear kinematic hardening law calibrated on the basis of the cyclic material properties derived from cyclic coupon tests performed by Kaufmann *et al*. (2001). The same cyclic material properties were used for the flanges and web of the links. Modelling of strength deterioration due to buckling has been taken into account by using the large displacements option. Previous studies (Richards and Uang 2005, Berman and Bruneau 2007) have shown that this approach is reliable.

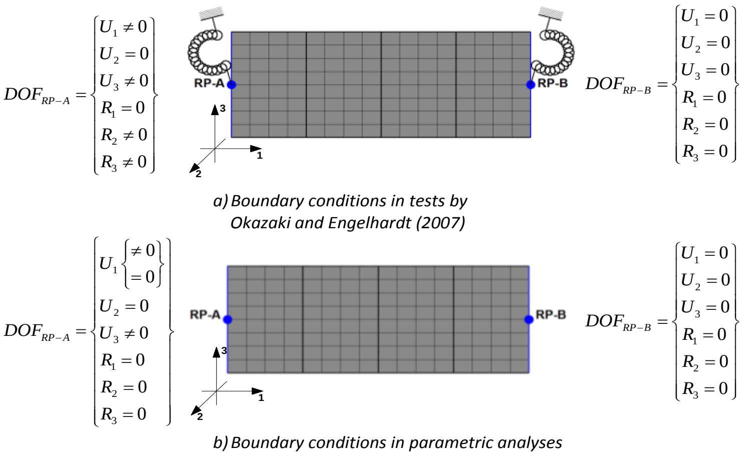

Figure 1. Boundary conditions in the FE Models.

Link boundary conditions are shown in Figure 1. Nodes belonging to cross-sections at the ends of the link were slaved to reference points: RP-A is the master node at one end and RP-B is the master node at the other end. The link shear deformation was imposed by applying a displacement at RP-A in the 3-direction (transverse to the link axis).
In order to reproduce accurately some tests results, linear rotational springs were needed to be introduced at link ends, as shown in Figure 1a. However, for the parametric analysis, perfect end restraints were assumed (Figure 1b). The cases $u_1 = 0$ (link with axial restraints) and $u_1 \neq 0$ (link without axial restraints) were alternatively considered.

2.2. Validation of finite element models

Accuracy of modelling assumptions was verified by comparison of theoretical outcomes with experimental results obtained by Okazaki and Engelhardt (2007). Out of the 37 links they investigated experimentally, the followings were examined: 1) W18 x 40 ($\frac{e \cdot V_p}{M_p} = 1.02$); 2) W10 x 33 ($\frac{e \cdot V_p}{M_p} = 1.04$); 3) W10 x 68 ($\frac{e \cdot V_p}{M_p} = 1.25$).

Material properties, stiffeners and loading protocols in the simulations are those of the experimental tests. Boundary conditions have been simulated to be as close as possible to the experimental setup. Hence, as illustrated in Figure 1a, flexural springs at both link ends have been included to simulate additional flexibility from boundary elements, namely the flexural stiffness of the members of the experimental frame which the links were connected to.

The results of numerical analyses showed a good agreement between the experimental and simulated response, both in terms of failure mechanism (Figure 2) and response curves (Figure 3). From comparison between numerical and experimental curves in Figures 3a, 3b, 3c it can be easily recognized that the monotonic response curves underestimate slightly the peak shear strength.

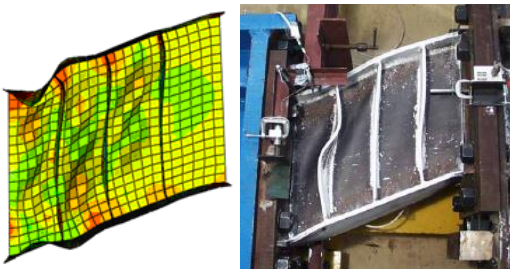

Figure 2. Numerical vs. experimental failure mode (W18x40).

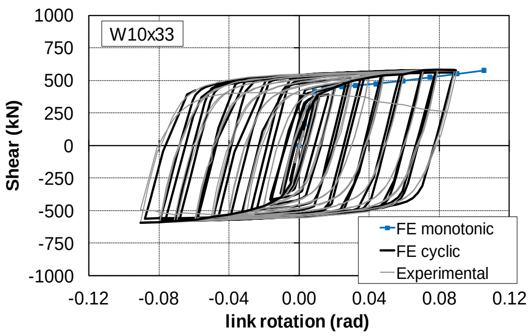

a)

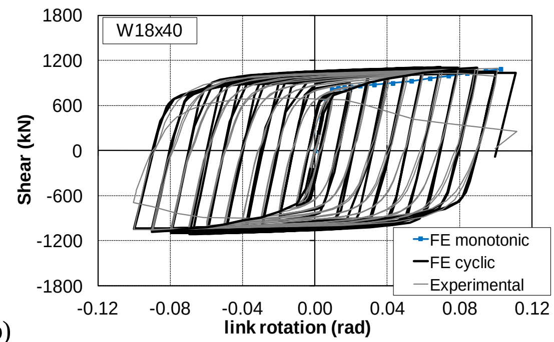

b)

Figure 3. Numerical vs. experimental response curves: W18x40 (a); W10x33 (b); W10x68 (c). (Continued)

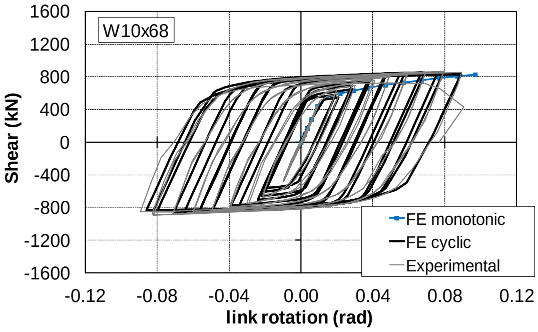

c)

Figure 3. Numerical vs. experimental response curves: W18x40 (a); W10x33 (b); W10x68 (c).

2.3. Parametric analysis

A parametric analysis has been carried out on shear links made of European hot-rolled shapes, namely HE A, HE B, HE M and IPE (with cross section depth ranging from 100 mm to 600 mm). The average stress-strain curve for the S 275 steel grade has been considered (Byfield *et al*. 2005). For each class of section shape, two ensembles of links have been considered with different lengths: $e_1 = 1.6 M_p / V_{y1}$ and $e_4 = 1.6 M_p / V_{y4}$, where: $V_{y1} = \frac{f_y}{\sqrt{3}} \cdot (d - 2t_f) \cdot t_w$ and $V_{y4} = \frac{f_y}{\sqrt{3}} \cdot A_{w,EC3}$ ($A_{w,EC3} = \left(A - 2b_f t_f + (t_w + 2r) \cdot t_f\right)$ is the shear area defined by Eurocode 3). It can easily be derived that $V_{y1} < V_{y4}$, hence $e_1 > e_4$. This choice was motivated by the idea to analyze the effect of axial restraints in a representative range of link lengths.

Figure 4a illustrates the link shear force (V) vs. rotation (γ) relationship obtained from the FE model analysis results for an ensemble of links with axial restraints. Results are relevant to HE A shapes with depth d of the cross section in the range (100 mm, 600 mm) and link lengths from 575 mm to 2112 mm. The results plotted in Figure 4 are all relevant to short links, i.e. links yielding in shear.

The axial force developed by the selected ensemble of HE A shapes is illustrated in Figure 4b. Comparing Figures 4a and 4b, it can be noted that the axial force is very small for small link rotations (let say smaller than 0.01 rad). But, the axial force rapidly increases for larger rotations reaching an intensity which is comparable to that of the shear force. Hence, it is argued that axial forces and their effects are not negligible in the plastic range of response.

Results similar to those illustrated here for HE A shapes can be obtained for other cross section types and link lengths. Further results from the parametric analysis are shown in the following Sections and utilized to derive a simple analytical model to capture the link plastic overstrength.

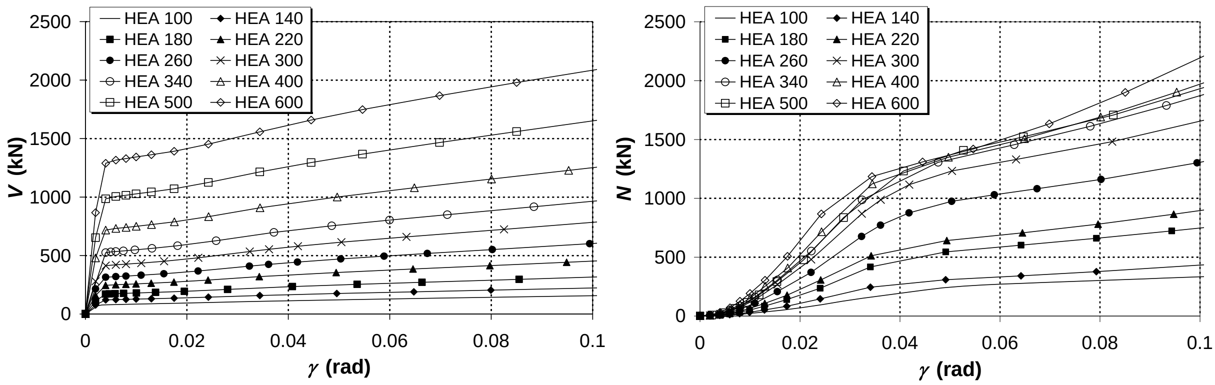

a) b)

Figure 4. Some FE model results for HEA shapes.

3. ANALYTICAL MODELLING OF SHEAR LINKS

3.1. Yielding limit state

Link elastic stiffness can be analytically computed using basic concepts of beam elastic mechanics. The second-order axial force developing as a consequence of the shear deformation is considered negligible in the elastic range of response (Figure 4).

Consequently, the elastic stiffness ($k_e = \frac{dV}{d\gamma}$) may be computed by means of Equation (1):

$$k_e = \frac{1}{\frac{1}{GA_w} + \frac{e^2}{12EI}} \tag{1}$$

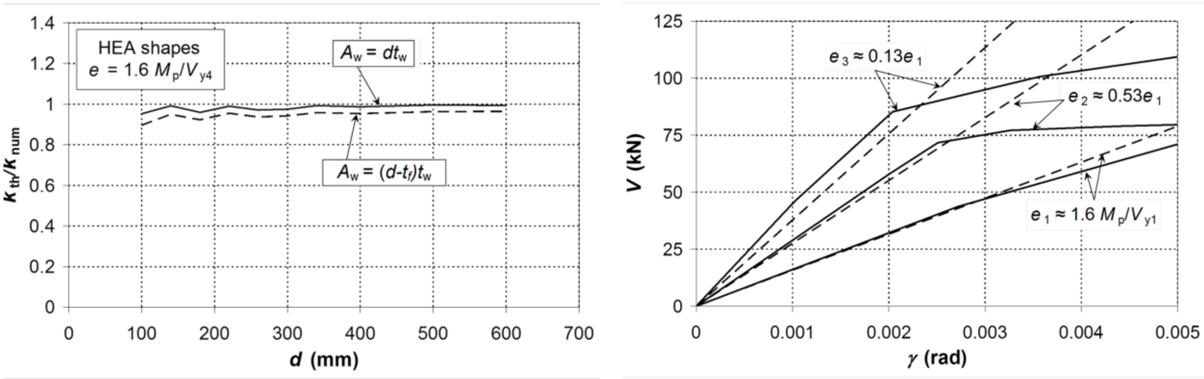

a) b)

Figure 5. Theoretical vs. numerical shear stiffness.

Figure 5a shows the ratio between the theoretical stiffness (k_{th}) corresponding to Eqn. (1) and the numerical value (k_{num}) obtained from the results of FE model analyses. Results for two alternative definitions of shear area are illustrated: $A_{w,1} = dt_w$ and $A_{w,2} = (d - t_f)t_w$. It can be seen that $A_{w,1} = dt_w$ gives the best approximation. Similar results have been obtained for other cross section shapes and lengths. However, it has been found that the approximation become worst when the link length reduces. This is illustrated by Figure 5b, where an HE A 100 shape and three different lengths are considered. This plot shows that the shear stiffness given by Eqn. (1) tends to underestimate the actual stiffness when very short links are considered. The correction of Eqn. (1) with the second order geometric stiffness due to the axial force has been checked to be negligible. Hence, the progressive deviation of the theoretical value from the numerical one must be attributed to the inapplicability of the beam theory for very small link lengths. Based on the numerical results, the approximation of a shear area equal to $A_w = dt_w$ is considered acceptable for link lengths larger than two times the cross section depth, i.e. $e > 2d$.

Several definitions are available in the technical literature for the shear yielding strength:

$$V_{y1} = \tau_y (d - 2t_f) t_w \tag{2}$$

$$V_{y2} = \tau_y (d - t_f) t_w \tag{3}$$

$$V_{y3} = \tau_y d t_w \tag{4}$$

$$V_{y4} = \tau_y A_{w,EC3} \tag{5}$$

where τ_y is the unit shear strength.

Eqn. (2) with $\tau_y = 0.6 f_y$ is used by AISC-341 (2010) for link strength calculation and classification, while Eqn. (3) is used for the same purposes by EN 1998-1 (2005) with $\tau_y = f_y / \sqrt{3}$. Some Authors (Popov and Engelhardt 1988, Bruneau et al. 1998) suggest the use of Eqn. (4), with $\tau_y = 0.55 f_y$. Eqn. (5) gives the plastic shear strength of I-shaped beams according to EN 1993:1-1 (2005), with $\tau_y = f_y / \sqrt{3}$.

In the following, the definition of the yield strength according to EN 1998-1 (2005) will be used for conventional calculations of overstrength ratios.

3.2. Ultimate limit state

Figure 6 shows a free body diagram of link forces (Della Corte et al. 2008, 2009a,b) for the more general case of a link with axial restraints. Accordingly, the increment of the shear force in the inelastic range (ΔV) is obtained from equilibrium as given by Eqn. (6):

$$\Delta V = \frac{\Delta M}{(e/2)} = \frac{\Delta N x}{(e/2)} \tag{6}$$

where:
– ΔN is the increase of the axial force after yielding (i.e. for $V > V_y$)
– x is the eccentricity of ΔN about the centroidal axis due to the corresponding increase of the first-order bending moment ($\Delta M = \Delta V \frac{e}{2}$) acting on the cross section at the link end ($x = \frac{\Delta M}{\Delta N}$).
It is noted that in case of no axial restraint, the axial force N is zero while the eccentricity x is infinite, so that the product (ΔM) is finite.

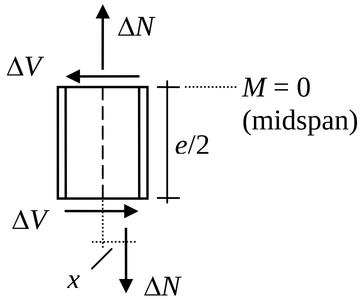

Figure 6. Free-body diagram of link incremental forces.

Therefore, using Eqn. (6) the link overstrength factor can be computed by means of Eqn. (7):

$$\frac{V}{V_y} = \frac{V_y + \Delta V}{V_y} = 1 + \frac{\Delta M}{V_y (e/2)} = 1 + \frac{\Delta N \cdot x}{V_y (e/2)} \tag{7}$$

Substituting $V_y = \left(f_y / \sqrt{3} \right) A_w$ into Eqn. (7), after some simple manipulation, Eqn. (8) is obtained:

$$\frac{V}{V_y} = 1 + 4\sqrt{3} \left(\frac{\Delta N}{2N_{fy}} \right) \left(\frac{x}{d} \right) \left(\frac{A_f}{A_w} \right) \left(\frac{d}{e} \right) \tag{8}$$

Using results of FE model analyses, it can be shown that both the normalized increase of axial force $\Delta n = \frac{\Delta N}{2N_{fy}}$ and its normalized location $\xi = \frac{x}{d}$ are functions of the normalized link length $\rho = e / \left(M_p / V_{y1} \right)$. The product $\Delta m = \Delta n \cdot \xi$ represents the normalized increase of bending moment. As previously noted, if the stiffness of the axial restraint approaches zero, then Δn approaches zero but ξ approaches infinite, so that Δm is still a finite quantity that can be measured.
Since Eqn. (8) requires knowledge of the product Δm rather than the individual factors (Δn and ξ), this product has been plotted in Figure 7. Very interestingly, Figure 7a shows that the variation of Δm is relatively small when links of length in the range $1.6 \frac{M_p}{V_{y4}} \le e \le 1.6 \frac{M_p}{V_{y1}}$ and axial restraints are considered. For example, at a link plastic rotation of 0.08 rad, the minimum value recorded for all the HE A shapes considered is 0.22 and the maximum value is 0.25. The average value is equal to 0.24 for

link lengths equal to $1.6\frac{M_{\rm p}}{V_{\rm y4}}$ and 0.25 for link lengths equal to $1.6\frac{M_{\rm p}}{V_{\rm y1}}$, thus demonstrating that the product Δm is quite insensitive to the normalized link length.
An attempt has been made to explore whether this property of an almost constant value of the product Δm remains valid outside of the investigated range of link lengths. To this end, a HE A 100 shape was considered, with length equal to $0.75\times 1.6\frac{M_{\rm p}}{V_{\rm y4}}$. Figure 7a shows that, unfortunately, this property seems to be not valid for shorter links. In other words, the ratio Δm appears to be reducing with the normalised link length, at a given plastic rotation, but with an initially negligible variation when the length is close to the limit value $1.6\frac{M_{\rm p}}{V_{\rm y1}}$. Indeed, the stiffness given by Eqn. (1) tends to underestimate the stiffness coming from FE models as far as the link length is reduced, the approximation being acceptable when the length is $e > 2d$. Analogously, the yielding shear strength given by one of the Eqns. (2), (3) or (4) tends to be an overestimation of the yielding point coming from FE model results, as far as the link length reduces. However, the approximations related to the beam theory are acceptable when links are considered with length in the range $1.6\frac{M_{\rm p}}{V_{\rm y4}} \le e \le 1.6\frac{M_{\rm p}}{V_{\rm y1}}$, where the ratio Δm appears also to be a rather stable quantity, whose variation may be neglected.
In case of links without axial restraints, the variation of the product Δm is relatively large. Indeed, at a link plastic rotation of 0.08 rad, the minimum value recorded for all the HE A shapes considered is 0.16 and the maximum value is 0.22, as shown in Figure 7b. The average value is equal to 0.17 for link lengths equal to $1.6\frac{M_{\rm p}}{V_{\rm y4}}$ and 0.19 for link lengths equal to $1.6\frac{M_{\rm p}}{V_{\rm y1}}$.
Neglecting the influence of this variation for Δm, for each type of link shape a constant value of Δm at $\gamma_{\rm p}$ = 0.08 rad could be assumed (Figure 7), with difference made between links with or without axial restraints. Thus Eqn. (9) is obtained:

$$\frac{V_{0.08}}{V_{\rm y}} = 1 + \beta_i \left(\frac{A_{\rm f}}{A_{\rm w}}\right)\left(\frac{d}{e}\right) \tag{9}$$

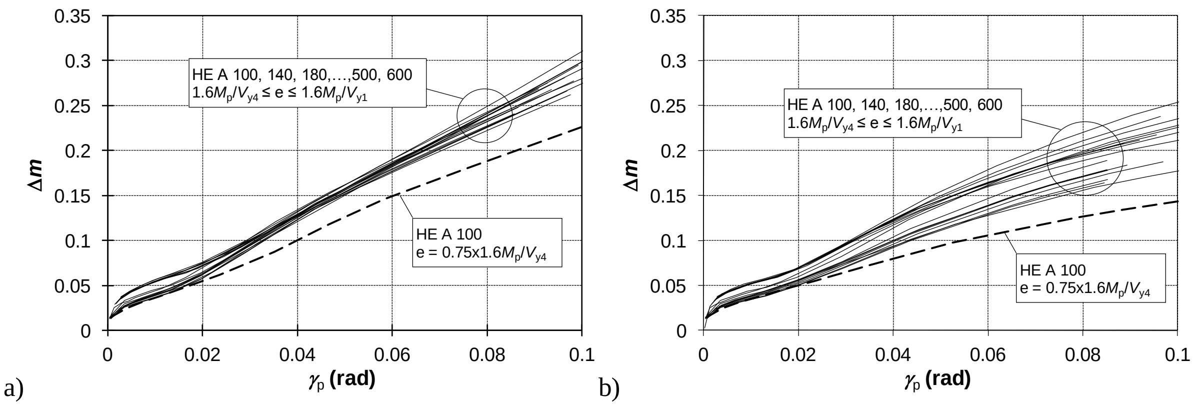

Figure 7. The variation of Δm: (a) with axial restraints; (b) without axial restraints.

Applying Eqn (9), for all European HE shapes and comparing the analytical predictions with the FE model results at $\gamma_{\rm p}$ = 0.08 rad, values of β_1 = 1.70 for links with axial restraints and β_2 = 1.35 for links without axial restraints have been found effective. For IPE shapes smaller variations of Δm have been observed for links with or without axial restraints, leading to suggest a value of β_1 = 1.70 (with axial restraints) and β_2 = 1.60 (without axial restraints). This result can be observed analyzing the plots in Figure 8, where the shear overstrength obtained by FE simulation for axially unrestrained and restrained links is compared to the analytical predictions for two ensembles of link lengths ($e_1 = 1.6 M_p / V_{y1}$ and $e_4 = 1.6 M_p / V_{y4}$). It is interesting to observe that the influence of axial restraints is noticeable for shorter links, while becoming less significant when link lengths approach the upper bound to short links (e_1).

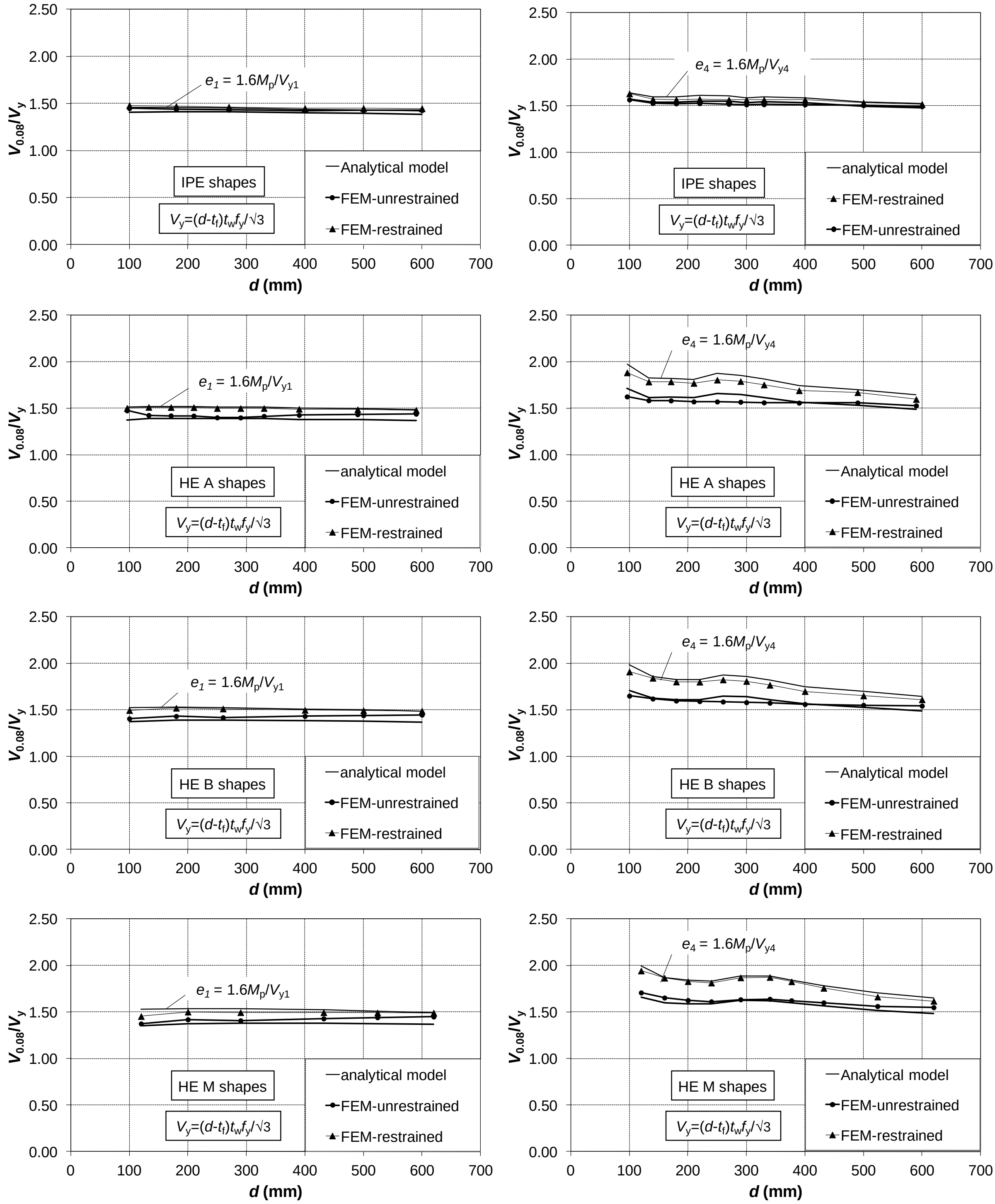

Figure 8. Comparison of analytical and FE model results.

3.3. Comparison with experimental data

Values of shear plastic overstrength experimentally measured during tests on short links having axial restraints have been collected from the available literature. Obviously, axial restraints in the experimental tests were characterized by finite stiffness. Therefore, experimental values are compared with the range of the analytical predictions (with and without axial restraints), as shown in Table 1. It is worth noting that the link plastic shear strength reported in references (Hjelmstad and Popov 1983, Stratan and Dubina 2002, Mazzolani *et al.* 2009, Dusicka *et al.* 2010) and used for the comparison were recalculated on the basis of Eqn. (4). Moreover, the comparison was made using the shear force experienced by the tested links at 0.08 radians of plastic deformation. As shown by Table 1, experimental results are within the range of analytical model predictions.

Table 1. Comparison of analytical results and experimental data.

Test results	Specimen	$(V_{0.08}/V_y)_{experimental}$	$(V_{0.08}/V_y)_{analytical}$	
			without axial restraints	with axial restraints
Hjelmstad & Popov (1983)	W18x40	1.60-1.66*	1.49	1.62
Dusicka *et al.* (2010)	Built-up	1.85	1.76	1.95
Mazzolani *et al.* (2009)	Built-up	2.20	1.98	2.24
Stratan *et al.* (2002)	IPE 240	1.58	1.53	1.67
*this range indicates the peak shear overstrength for positive and negative deformation.				

4. CONCLUSIONS

A theoretical study about the response of shear links has been carried out. The study is essentially based on FE model analysis, but comparison with experimental test results has also been considered. Based on both the experimental evidence and the numerical results of FE models, the following conclusions are drawn:

1. Three basic parameters may have a combined effect on link shear overstrength: (i) axial forces, (ii) the ratio of flange over web area and (iii) the ratio of link length and cross section depth.
2. It has been noted that tensile axial forces may develop due to axial restraints and nonlinear geometric effects. These tensile forces acting in combination with the other two parameters may significantly modify the link shear overstrength.
3. An analytical model for predicting the overstrength of shear links with or without axial restraints has been proposed taking into account the above three parameters. The larger is the area of flanges and the shorter is the link, the larger is the link shear force developing at a given link rotation, for given boundary conditions.
4. In usual cases, an overstrength ratio equal to 1.5 has been confirmed by the theoretical investigation. However, for very short links, with compact cross sections and perfect axial restraints, values of shear overstrength up to 2 have been obtained in the range of shapes and lengths investigated. For built-up links with very compact shape and short length, even larger values could be obtained.
5. Comparison of theoretical predictions and experimental test results indicates the ability of the proposed model to correctly capture the range of shear overstrength values corresponding to different degrees of axial restraint.

ACKNOWLEDGEMENT
The financial support of the Italian Ministry for Research and Education (MIUR), within Grant PRIN 2005-2007 "Advanced steel braces with uncoupled design parameters", is gratefully acknowledged.

Authors are sincerely grateful to Dr. T. Okazaki and Professor Michael Engelhardt, who provided their experimental results from tests performed at the University of Texas at Austin.

REFERENCES

American Institute of Steel Construction, Inc. (AISC) (2010). *Seismic provisions for structural steel buildings. Standard ANSI/AISC 341-10*. Chicago (IL, USA).

ABAQUS user's manual, 2010, Dassault Systèmes Simulia Corp., Providence, RI, USA.

Berman J. W., Bruneau M. (2007). Experimental and analytical investigation of tubular links for eccentrically braced frames. *Engineering Structures* **29**, 1929–1938

Bruneau M., Uang C. M., Whittaker A. (1998). *Ductile design of steel structures.* McGraw-Hill, USA.

Byfield M. P., Davies J. M., Dhanalakshmi M. (2005). Calculation of the strain hardening behaviour of steel structures based on mill tests. *Journal of Constructional Steel Research*, **61**, 133-150.

D'Aniello M. (2006). Seismic upgrading of RC structure by steel Eccentric Bracing: an experimental and numerical study. *Pollack Periodica*, **1:2**, 3–15.

Della Corte G., D'Aniello M., Mazzolani F.M., (2008). Plastic shear over-strength of short links: the effects of axial restraints. *Proc. of 5th European Conference on Steel and Composite Structures*, Graz, 3-5 Sept.

Della Corte G., D'Aniello M., Mazzolani F. M. (2009). Plastic shear overstrength of short links with axial restraints. *Proceedings of STESSA 2009. Conference – Steel Structures in Seismic Area*. Philadelphia (USA), 16-20 August.

Della Corte G., D'Aniello M., Mazzolani F. M. (2009). Advanced steel bracing systems: Experimental tests and analytical models. In: *"Innovative strategies for structural protection of built heritage",* Monza (Milan, Italy): Polimetrica, 347-398.

Dusicka P., Itani A. M., Buckle I.G. (2010). Cyclic Behavior of Shear Links of Various Grades of Plate Steel. *Journal of Structural Engineering*, **136:4**.

European Committee for Standardization (CEN) (2005). Eurocode 8 – *Design of structures for earthquake resistance – Part 1.1: General rules, seismic actions and rules for buildings*. EN 1998-1-1, Bruxelles.

European Committee for Standardization (CEN) (2005). Eurocode 3 – *Design of steel structures – Part 1.1: General rules and rules for buildings*. EN 1993-1-1, Bruxelles.

Hjelmstad K. D., Popov E. P. (1983). Cyclic behaviour and design of link beams. *Journal of Structural Engineering – ASCE*, **109:10**, 2387-2403.

Kasai K., Popov E. P. (1986). General behaviour of WF steel shear link beams. *Journal of Structural Engineering – ASCE*, **112:2**, 362-382.

Kaufmann E. J., Metrovich B. R., Pense A. W. (2001). Characterization of cyclic inelastic strain behavior on properties of A572 Gr. 50 and A913 Gr. 50 rolled sections. *ATLSS Report* No. 01-13, Lehigh Univ., Bethlehem, Pa.

Malley J. O., Popov E. P. (1984). Shear Links in Eccentrically Braced Frames. *Journal of Structural Engineering*, **110:9**, 2275-2295.

Mazzolani F. M., Della Corte G., D'Aniello M. (2009). Experimental analysis of steel dissipative bracing systems for seismic upgrading. *Journal of Civil Engineering and Management* **15:1**, 7-19.

McDaniel C. C., Uang C. M., Seible F. (2003). Cyclic testing of built-up steel shear links for the new bay bridge. *Journal of Structural Engineering - ASCE*, **129:6**, 801-809.

Okazaki T., Engelhardt M. D. (2007). Cyclic loading behavior of EBF links constructed of ASTM A992 steel. *Journal of constructional Steel Research*, **63**, 751-765.

Popov E. P., Malley J. O. (1983). Design of links and beam-to-column connections for eccentrically braced steel frames. *Report No. UCB/EERC-83/03*, January, Earthquake Engineering Research Center, University of California, Berkeley.

Popov E. P., Engelhardt M. D. (1988). Seismic eccentrically braced frames. *Journal of Constructional Steel Research*, **10**, 321-354.

Richards P., Uang C. M. (2005). Effect of Flange Width-Thickness Ratio on eccentrically Braced Frames Link Cyclic Rotation Capacity. *Journal of Structural Engineering*, **131:10**.

Richards P., Uang C. M. (2006). Testing Protocol for Short Links in Eccentrically Braced Frames. *Journal of Structural Engineering*, **132:8**, August 1.

Ricles J. M., Popov E. P. (1987). Dynamic analysis of seismically resistant eccentrically braced frames. *Earthquake Engineering Research Center*, University of California, Berkeley.

Roeder C. W., Popov E. P. (1978). Eccentrically braced steel frames for earthquakes. *Journal of the Structural Division – ASCE*, **104:3**, 391-412.

Saritas A., Filippou F. C. (2004). Modelling of shear-yielding members for seismic energy dissipation. *Proceedings of the 13th World Conference on Earthquake Engineering*, Vancouver, Canada, CD-ROM: paper no. 1799.

Stratan A., Dubina D. (2002). Seismic performance of eccentric braced frames with removable low yield steel link. *Proceedings of International Conference Earthquake Loss Estimation and Risk Reduction*, 117-127, Bucureşti (România), 24-26 October.